Featured Article

Targeting the Platelet-Derived Growth Factor Receptor in Antivascular Therapy for Human Ovarian Carcinoma

Sachin M. Apte,[1,2] Dominic Fan,[1] Jerald J. Killion,[1] and Isaiah J. Fidler[1]

Departments of [1]Cancer Biology and [2]Gynecologic Oncology, The University of Texas M. D. Anderson Cancer Center, Houston, Texas

Abstract

Purpose: **We sought to determine whether blockade of platelet-derived growth factor receptor (PDGF-R) activation by oral administration of a PDGF-R tyrosine kinase inhibitor (STI571) alone or in combination with i.p. paclitaxel can inhibit the progression of tumors caused by human ovarian carcinoma cells growing in the peritoneal cavity of female nude mice.**

Experimental Design: **In several different experiments, paclitaxel-sensitive and paclitaxel-resistant metastatic human ovarian carcinoma cells were injected into the peritoneal cavity of nude mice. Seven days later, groups ($n = 10$) of mice began receiving a control treatment, STI571 alone, paclitaxel alone, or a combination of STI571 and paclitaxel. The mice were necropsied after 45 days of treatment.**

Results: **Treatment with combination therapy significantly reduced tumor weight (relative to control or single-agent therapy) in all three human ovarian cancer cell lines. Immunohistochemical analyses revealed that PDGF-R activation was blocked by STI571 administered alone or in combination with paclitaxel. Tumor-associated endothelial cells expressed both PDGF-R and phosphorylated PDGF-R. In mice receiving combination therapy, tumor-associated endothelial cells underwent apoptosis, leading to decreases in microvessel density and tumor cell proliferation relative to control and single-agent therapy.**

Conclusions: **These results show that administration of a PDGF-R tyrosine kinase inhibitor in combination with paclitaxel impairs the progression of ovarian cancer in the peritoneal cavity of nude mice, in part, by blockade of PDGF, an endothelial cell survival factor, which results in the increased apoptosis of tumor-associated endothelial cells.**

Received 7/31/03; revised 9/26/03; accepted 9/30/03.

Grant support: Cancer Center Support Core Grant CA16672 and SPORE in Ovarian Cancer Grant CA93639 from the National Cancer Institute, NIH.

The costs of publication of this article were defrayed in part by the payment of page charges. This article must therefore be hereby marked *advertisement* in accordance with 18 U.S.C. Section 1734 solely to indicate this fact.

Requests for reprints: Isaiah J. Fidler, Department of Cancer Biology, Unit 173, The University of Texas M. D. Anderson Cancer Center, 1515 Holcombe Boulevard, Houston, TX 77030. Phone: (713) 792-8577; Fax: (713) 792-8747; E-mail: ifidler@mdanderson.org.

Introduction

According to the American Cancer Society, an estimated 25,400 new cases of ovarian cancer will occur in the United States in 2003 (1). Ovarian cancer is the second most common malignant neoplasm of the female genital tract in the United States but is the leading cause of gynecologic cancer death (1). Because no effective screening tool exists for the general population and the disease is notorious for a lack of early warning signs, the majority of patients present with metastatic disease. The advent of modern surgical techniques and platinum-based chemotherapy did not affect ovarian cancer mortality from 1979 to 1995 (2). Despite initial tumor response rates of 80% to front-line platinum-based chemotherapy (3), the majority of patients with advanced ovarian cancer will ultimately have cancer relapse and develop drug-resistant disease (4, 5). Currently available second-line agents, all of which have associated response rates of ~15–25%, include doxil, topotecan, gemcitabine, oral etoposide, tamoxifen, and vinorelbine (6). Because recurrent and progressive epithelial ovarian cancers have a relatively low response rate to all known active agents, there is a critical need for a better understanding of ovarian cancer biology to allow the development of better therapy.

The expression of platelet-derived growth factor (PDGF) and PDGF receptor (PDGF-R) has been associated with a variety of human neoplasms, including those of the prostate (7–11), lung (12), colon (13), and breast (14, 15). PDGF is the cellular homologue of v-*sis* and causes transformation *in vitro* (16). Stimulation of autocrine PDGF is thought to contribute to the early transformation and progression of glioblastoma (17, 18), melanoma, pancreatic cancer, and prostate cancer (19).

Several published studies implicate PDGF and PDGF-R in ovarian cancer growth. PDGF-Rα and PDGF-Rβ are present on HOSE cells, and PDGF has been shown to enhance the growth of HOSE cells *in vitro* (20). Also, while the normal ovary epithelium and benign ovarian neoplasms do not express PDGF and PDGF-Rα, 73% of ovarian carcinomas express PDGF and 36% express PDGF-Rα (21). Moreover, expression of PDGF-Rα is an independent poor prognostic factor in ovarian carcinoma (21). A recent study reported that six epithelial ovarian cancer cell lines expressed the PDGF A- and B-chain genes and that PDGF was expressed in frozen sections of six serous ovarian carcinomas (22). Collectively, these data suggest a possible role for PDGF and PDGF-R in the progression of ovarian cancer.

STI571, a derivative of 2-phenylaminopyrimidine, was originally developed as a competitor for an ATP-binding site of the Abl protein tyrosine kinase (23). STI571 is also a potent tyrosine kinase inhibitor of c-Kit and PDGF-R (24–29). The purpose of the present study was to evaluate whether blockade of PDGF-R activation by STI571 can decrease the progressive growth of human ovarian cancer cells implanted into the peritoneal cavity of nude mice. We show that daily oral administrations of STI571 combined with weekly i.p. injections of

paclitaxel produced significant therapeutic effects, mediated in part by the induction of apoptosis in tumor-associated endothelial cells.

Materials and Methods

Ovarian Cancer Cell Lines and Culture Conditions. For these studies, we used the highly metastatic human ovarian cancer cell lines Hey A8 (30–32) and SKOV3ip1 (33, 34). The tumorigenic SKOV3ip1 line was established in culture from peritoneal metastases produced by the SKOV3 cells growing orthotopically in athymic mice (35). Hey A8 and SKOV3ip1 cells were grown as monolayer cultures in culture minimal essential medium (Life Technologies, Inc., Grand Island, NY), supplemented with 10% fetal bovine serum, vitamins, sodium pyruvate, L-glutamine, nonessential amino acids (Life Technologies, Inc.), and penicillin-streptomycin (Flow Laboratories, Rockville, MD). Adherent monolayers were maintained on plastic and incubated at 37°C in a mixture of 5% CO_2 and 95% air. The tumor cells were free of *Mycoplasma* and pathogenic murine viruses (assayed by M. A. Bioproducts, Walkersville, MD). The cultures were maintained for no longer than 12 weeks after recovery from frozen stock.

The Hey A8 paclitaxel-resistant line was selected from the parental Hey A8 cell line by culturing the cells in culture minimal essential medium containing increasing concentrations of paclitaxel. After 18 months, the derived cells were resistant to 500 ng/ml paclitaxel.

Reagents. Primary antibodies were purchased as listed: goat anti-phosphorylated (*p*)-PDGF-Rα (Tyr^{720}; Santa Cruz Biotechnology, Santa Cruz Biotechnology, CA); goat anti-*p*-PDGF-Rβ (Tyr^{1021}; Santa Cruz Biotechnology); rabbit anti-PDGF-Rα (C-20; Santa Cruz Biotechnology); rabbit anti-PDGF-Rβ (958; Santa Cruz Biotechnology); rabbit anti-PDGF-A (N-30; Santa Cruz Biotechnology); rabbit anti-PDGF-B (N-30; Santa Cruz Biotechnology); rat antimouse CD31 (BD PharMingen, San Diego, CA); and mouse anti-proliferating cell nuclear antigen (PCNA) clone PC 10 (Dako A/S, Copenhagen, Denmark). The following secondary antibodies were used for colorimetric immunohistochemistry (IHC) analysis: peroxidase-conjugated goat antirabbit IgG; F(ab′)2 (Jackson ImmunoResearch Laboratories, Inc., West Grove, PA); biotinylated mouse antigoat (Biocare Medical, Walnut Creek, CA); streptavidin horseradish peroxidase (Dako A/S); rat antimouse IgG2a horseradish peroxidase (Serotec, Harlan Bioproducts for Science, Inc., Indianapolis, IN); and goat antirat horseradish peroxidase (Jackson ImmunoResearch Laboratories, Inc., West Grove, PA). The following fluorescent secondary antibodies were used: Alexa 488-conjugated goat antirabbit IgG (Molecular Probes, Inc., Eugene, OR); Alexa 488-conjugated rabbit antigoat IgG (Molecular Probes); Texas Red-conjugated goat antirat IgG (Jackson ImmunoResearch Laboratories); Alexa 488-conjugated goat antirat IgG (Molecular Probes); and Rhodamine Red donkey antirat IgG (Jackson ImmunoResearch Laboratories). Terminal deoxynucleotidyl transferase-mediated nick end labeling (TUNEL) staining was performed using a commercial apoptosis detection kit (Promega, Madison, WI) with modifications. Other reagents included Hoechst 3342 dye (Polysciences, Inc., Warrington, PA), stable 3,3′-diaminobenzidine (Research Genetics, Huntsville, AL), Gill's hematoxylin (Sigma Chemical Co., St. Louis, MO), cold water fish skin gelatin 40% (Electron Microscopy Sciences, Fort Washington, PA), and propyl gallate (ACROS Organics, Morris Plains, NJ).

STI571 [imatinib mesylate (Gleevec), Novartis, Basel, Switzerland] is a small-molecule inhibitor of the tyrosine kinases PDGF-R, c-Kit, and Bcr-Abl (24–29). For oral administration, STI571 was dissolved in distilled water at 6.25 mg/ml and prepared daily.

Paclitaxel (Taxol; Bristol-Myers Squibb Co., Princeton, NJ) is a poorly soluble plant product from the western yew, *Taxus brevifolia*. A sterile solution concentrate is available at 6 mg/ml in 5-ml vials (30 mg/vial) in 50% polyoxyethylated castor oil and 50% dehydrated alcohol, USP. The concentrate was diluted in distilled water at 625 μg/ml and prepared just before use.

***In Vitro* Blockade of PDGF-R Phosphorylation.** SKOV3ip1 and Hey A8 cells were plated at a density of 7.5×10^3 cells/cm^2 on tissue culture-treated glass slides (Becton Dickinson and Company, Franklin Lakes, NJ) in a two-chamber polystyrene vessel containing medium with 10% fetal bovine serum. Hey A8 paclitaxel-resistant cells were plated at a density of 10^4 cells/cm^2. The following day, the medium was replaced with serum-free culture minimal essential medium containing different concentrations of STI571. Twenty-four h later, the cells were stimulated for 15 min with PDGF-BB at 10 ng/ml. The chambers were washed and the slides were fixed and stained as described below.

IHC Determination of PDGF-R and *p*-PDGF-R Expression on Human Ovarian Carcinoma Cells Growing in Culture. The slides with attached cells were fixed in cold acetone for 10 min and then washed twice with PBS for 3 min each time. Slides were placed in a humidified chamber and incubated with a protein blocking solution (PBS supplemented with 4% cold water fish skin gelatin). Samples were then incubated overnight at 4°C with a 1:100 dilution of anti-PDGF-R or anti-*p*-PDGF-R primary antibody. The slides were then rinsed three times with PBS and incubated for 10 min in protein blocking solution. For PDGF-R staining, the samples were incubated with a peroxidase-conjugated goat antirabbit antibody for 1 h at room temperature (1:1000 dilution). For *p*-PDGF-R staining, the slides were first treated with a biotinylated mouse antigoat antibody for 30 min (prediluted), followed by streptavidin horseradish peroxidase for 30 min (1:300 dilution). The samples were then rinsed three times in PBS. Positive reactions were rendered visible by incubating the slides with stable 3,3′-diaminobenzidine for 5–10 min. The sections were rinsed with distilled water, counterstained with Gill's hematoxylin for 30 s, and mounted with Universal Mount (Research Genetics). Control samples exposed to secondary antibody alone showed no nonspecific staining.

***In Vitro* Proliferation Assay.** Tetrazolium (MTT) (M2128) was purchased from Sigma Chemical Co., and a stock solution was prepared by dissolving 5 mg of MTT in 1 ml of PBS and filtering the solution to remove particulates. The solution was protected from light, stored at 4°C, and used within 1 month. In the assay, ovarian cancer cells were plated in 96-well plates (Becton Dickinson) in triplicate and allowed to adhere overnight. STI571, paclitaxel, or both were then added in

dilution with serum-free culture minimal essential medium. The cells were exposed to paclitaxel in a range of concentrations, whereas the concentration of STI571 was constant. After 96 h, the number of metabolically active cells was determined by the MTT assay (36).

Animals. Female athymic nude mice (NCr-*nu*) were purchased from the Animal Production Area of the National Cancer Institute-Frederick Cancer Research and Development Center (Frederick, MD). The mice were housed and maintained under specific-pathogen-free conditions in facilities approved by the American Association for Accreditation of Laboratory Animal Care and in accordance with current regulations and standards of the United States Department of Agriculture, the United States Department of Health and Human Services, and the NIH. The mice were used in these experiments according to institutional guidelines when they were 8–12 weeks old.

Orthotopic Implantation of Tumor Cells and Necropsy Procedures. To produce tumors, SKOV3ip1, Hey A8, and Hey A8 paclitaxel-resistant cells were harvested from subconfluent cultures by a brief exposure to 0.25% trypsin and 0.02% EDTA. Trypsinization was stopped by replacing the trypsin-EDTA with medium containing 10% fetal bovine serum, and the cells were washed once in serum-free medium and resuspended in HBSS. Only single-cell suspensions with >95% viability, determined by Trypan Blue exclusion, were used for the *in vivo* injections. To test the effects of the therapies, SKOV3ip1 and Hey A8 paclitaxel-resistant cells were injected i.p. into female nude mice at a concentration of 1×10^6 cells/0.2 ml HBSS; Hey A8 cells were injected i.p. at a concentration of 2.5×10^5 cells/0.2 ml HBSS into female nude mice.

Mice were killed on day 45 of the study and weighed. Primary tumors in the peritoneal cavity were excised and weighed. In animals bearing SKOV3ip1 tumors, malignant ascites were aspirated and measured. For IHC and H&E-staining procedures, tumors were fixed in formalin and embedded in paraffin. For IHC requiring frozen tissue, tumors were embedded in OCT compound (Miles, Inc., Elkhart, IN), frozen rapidly in liquid nitrogen, and stored at −80°C.

Therapy for Established Human Ovarian Carcinoma Growing in the Peritoneal Cavity of Female Nude Mice. To evaluate the therapeutic effect of combination therapy in the animal model, we first performed preliminary dose-response experiments for both STI571 and paclitaxel. To determine the optimal dose of STI571, Hey A8 cells were implanted i.p. Fourteen days after the orthotopic implantation of tumor cells, mice were randomized into four groups ($n = 6$/group): PBS p.o. or STI571 at 25, 50, or 100 mg/kg/day p.o. Mice were treated for 5 consecutive days. Two, 12, and 24 h after administration of the last oral treatment, 2 mice/group were killed. Fluorescence IHC was performed on the tumors as described below. Preliminary survival experiments using paclitaxel alone were performed to determine an effective low dose for paclitaxel therapy (data not shown).

On the basis of these preliminary findings, we initiated a series of three separate therapy experiments. Tumor cells were injected i.p. Seven days later, the mice were randomized into four groups ($n = 10$ in each): daily PBS p.o. plus weekly PBS i.p.; 125 μg i.p. paclitaxel once/week; daily administration of 50 mg/kg p.o. STI571; and 125 μg of i.p. paclitaxel once/week plus daily 50 mg/kg p.o. STI571.

Immunofluorescence IHC. Expression of PDGF-Rα, PDGF-Rβ, *p*-PDGF-Rα, and *p*-PDGF-Rβ was determined on frozen samples from orthotopically growing tumors produced by Hey A8, SKOV3ip1, and Hey A8 paclitaxel-resistant cells. Fresh frozen tissues were cut into 4-μm sections and mounted on positively charged slides. The sections were stored at −80°C. Sections were fixed in cold acetone for 10 min, followed by two washes with PBS for 3 min each. Slides were placed in a humidified chamber and incubated with the protein blocking solution for 20 min at room temperature. Samples were then incubated overnight with an anti-PDGF-R or anti-*p*-PDGF-R primary antibody at 4°C. The slides were then rinsed three times with PBS, incubated 10 min in protein blocking solution, and incubated with Alexa 488-conjugated goat antirabbit IgG (for PDGF-R, 1:600 dilution) or Alexa 488-conjugated rabbit antigoat IgG (for *p*-PDGF-R, 1:600 dilution) secondary antibodies for 1 h at room temperature. The samples were then rinsed three times in PBS. Nuclear counterstain (Hoechst) was then applied for 2 min (1:2000 dilution). Samples were then rinsed three times in PBS, mounting medium was placed on each sample, and a glass coverslip (Fischer Scientific, Fair Lawn, NJ) was placed on top. Mounting medium consists of 90% glycerol, 10% PBS, and 0.1 M propyl gallate.

Immunofluorescence Double Staining for CD31 and PDGF-R or *p*-PDGF-R. Fresh frozen tissues were cut into 4-μm sections and mounted on positively charged slides. Sections were stored at −80°C. Sections were fixed in cold acetone for 10 min and then washed twice with PBS for 3 min each time. The slides were placed in a humidified chamber and incubated with protein blocking solution for 20 min at room temperature. Samples were then incubated overnight with rat antimouse CD31 antibody (1:800 dilution) at 4°C. The slides were then rinsed three times with PBS and incubated for 10 min in protein blocking solution. Slides for PDGF-R/CD31 staining were incubated with Alexa 594-conjugated goat antirat IgG (1:400 dilution) for 1 h at room temperature. Slides for *p*-PDGF-R/CD31 staining were incubated with Rhodamine Red donkey antirat IgG (1:50 dilution) for 1 h at room temperature. From this point, the slides were protected from light. Next, all slides were rinsed three times with PBS, incubated for 10 min in protein blocking solution, and then incubated with an anti-PDGF-R or anti-*p*-PDGF-R primary antibody overnight at 4°C (1:100 dilution). The slides were then rinsed three times with PBS, incubated for 10 min in protein blocking solution, and incubated with the corresponding fluorescent secondary antibody (Alexa 488-conjugated goat antirabbit for CD31/PDGF-R IHC and Alexa 488-conjugated rabbit antigoat for CD31/*p*-PDGF-R IHC) for 1 h at room temperature (1:500 dilution). The samples were then rinsed three times in PBS. Hoechst nuclear counterstain was applied for 2 min. Samples were then rinsed three times in PBS, mounting medium was placed on each slide, and the slides were covered with glass coverslips (Fischer Scientific).

Immunofluorescence Double Staining for CD31 and TUNEL. Frozen tissue was used for CD31/TUNEL immunofluorescence double staining. The procedure used is as described previously (37, 38). Endothelial cells were identified by red

fluorescence, and DNA fragmentation was detected by localized green fluorescence within the nucleus of apoptotic cells. An endothelial cell undergoing apoptosis was represented by yellow fluorescence (37).

IHC Determination of CD31 and PCNA. Expression of PCNA was determined by IHC using paraffin-embedded tumors. Sections (8-μm thick) were mounted on positively charged Superfrost slides (Fisher Scientific Co., Houston, TX) and dried overnight. Sections were deparaffinized in xylene, treated with a graded series of alcohol [100%, 95%, 80% ethanol/double distilled H_2O (v/v)], and rehydrated in PBS (pH 7.5). Antigen was retrieved by placing the slides in water and then boiling them in a microwave on high power for 5 min. Expression of CD31 was determined on fresh frozen tissues that were cut into 4-μm thick sections and mounted on positively charged slides. The slides were stored at −80°C; sections were fixed in cold acetone for 10 min and then washed twice with PBS for 3 min each time. Detection of PCNA and CD31 was carried out as described previously (38).

Quantification of Microvessel Density (MVD), PCNA, and CD31/TUNEL$^+$ Endothelial Cells. To quantify MVD, 10 random 0.159-mm^2 fields at ×100 magnification were examined for each tumor, and the microvessels within those fields counted. A single microvessel was defined as a discrete cluster or single cell stained positive for CD31 (CD31$^+$), and the presence of a lumen was not required for scoring as a microvessel. To quantify PCNA expression, the number of positive cells was counted in 10 random 0.159-mm^2 fields at ×100 magnification. To quantify CD31/TUNEL$^+$ cells, the number of double-positive cells was counted in 10 random 0.011-mm^2 fields at ×400 magnification.

Microscopy. 3,3′-Diaminobenzidine-stained sections were examined with a ×20 objective on a Nikon Microphot-FX microscope (Nikon, Inc., Garden City, NY) equipped with a three-chip charge-coupled device color video camera (Model DXC990; Sony Corp., Tokyo, Japan). Immunofluorescence microscopy was performed using a ×20 objective on a Nikon Microphot-FXA microscope (Nikon, Inc.) equipped with a HBO 100 mercury lamp and narrow band pass filters to individually select for green, red, and blue fluorescence (Chroma Technology Corp., Brattleboro, VT). Images were captured using a cooled charge-coupled device Hamamatsu 5810 camera (Hamamatsu Corp., Bridgewater, NJ) and Optimas Image Analysis software (Media Cybernetics, Silver Spring, MD). Photomontages were prepared using Micrografx Picture Publisher (Corel, Inc., Dallas, TX) and Adobe PhotoShop software (Adobe Systems, Inc., San Jose, CA). Photomontages were printed on a Sony digital color printer (Model UP-D7000). Endothelial cells were identified by red fluorescence, whereas PDGF-R and *p*-PDGF-R were identified by green fluorescence. Images were subsequently superimposed digitally, and endothelial cells expressing these receptors were identified by yellow fluorescence.

Statistical Analyses. Comparisons of mean tumor weight, volume of ascites, body weight, and mean MVD, PCNA, and TUNEL$^+$ cells were analyzed using two-tailed nonparametric tests (Mann-Whitney tests). Survival curve comparisons were performed using the log-rank test.

Results

***In Vitro* Cytostasis Mediated by Paclitaxel and STI571.** The human ovarian cancer cells (SKOV3ip1, Hey A8, and Hey A8 paclitaxel resistant) were cultured for 4 days in media containing various concentrations of paclitaxel in the absence or presence of a noncytostatic concentration of STI571 (4 μM). The growth inhibition mediated by paclitaxel was enhanced by STI571. For SKOV3ip1, Hey A8, and Hey A8 paclitaxel-resistant cells, the IC_{50} for paclitaxel, as determined by the MTT assay, decreased from 1.0, 0.7, and 600 ng/ml to 0.3, 0.2, and 100 ng/ml, respectively, in the presence of STI571.

Inhibition of PDGF-R Phosphorylation in Human Ovarian Cancer Cells by STI571. In the first set of experiments, we determined whether treatment of SKOV3ip1, Hey A8, or Hey A8 paclitaxel-resistant cells with STI571 could inhibit PDGF-BB-stimulated tyrosine phosphorylation of PDGF-R. Human ovarian cancer cells incubated for 15 min with serum-free medium containing PDGF-BB at 10 ng/ml expressed *p*-PDGF-R. The cells were incubated with different concentrations of STI571. PDGF-R expression was unaffected by STI571, but phosphorylation of the receptor in cells incubated with PDGF-BB was inhibited by STI571 at concentrations of 2–4 μM.

In the next set of experiments, we determined the dose of STI571 required to inhibit phosphorylation of the PDGF-R in cells growing *in vivo*. Human ovarian cancer cells were injected into the peritoneal cavity of mice. Two weeks later, groups of mice were treated daily p.o. with 0, 25, 50, or 100 mg/kg STI571. Two mice each were killed at 2, 12, and 24 h after the fifth daily treatment. The tumors were processed for IHC. Tumors expressed both PDGF-Rα and PDGF-Rβ. The expression of these receptors was not affected by STI571 (data not shown). Expression of *p*-PDGF-Rα is shown in Fig. 1. Treatment with STI571 at 25 mg/kg did not inhibit phosphorylation of the receptors. STI571 at 50 mg/kg was sufficient to reduce PDGF-R phosphorylation for up to 12 h. Twenty-four h after treatment, the PDGF-R was phosphorylated, suggesting that a dose of 50 mg/kg is the lowest effective daily dose.

Inhibition of Ovarian Cancer Growth in the Peritoneal Cavity of Nude Mice. The SKOV3ip1, Hey A8, or Hey A8 paclitaxel-resistant cells were implanted into the peritoneal cavity of athymic nude mice. Seven days later, the mice were randomized into four treatment groups of 10 mice each. The first group received daily saline p.o. and weekly saline i.p. The second group received a weekly i.p. injection of 125 μg of paclitaxel (because preliminary survival studies demonstrated that the lowest effective dose for paclitaxel in the ovarian cancer model was 125 μg i.p. once/week). The third group received daily p.o. STI571 (50 mg/kg), and the fourth group received daily p.o. STI571 (50 mg/kg) and weekly i.p. paclitaxel (125 μg). The data for these therapies' effects on SKOV3ip1, Hey A8, and Hey A8 paclitaxel-resistant cells are summarized in Tables 1, 2, and 3, respectively

Table 1 shows that STI571 therapy alone was not effective against SKOV3ip1 tumors. Paclitaxel alone was effective at reducing tumor weight and eliminating ascites. The combination of paclitaxel and STI571 reduced the incidence of tumor, further reduced tumor weight, and also eliminated ascites; the reduction in tumor weight was statistically significant compared with all

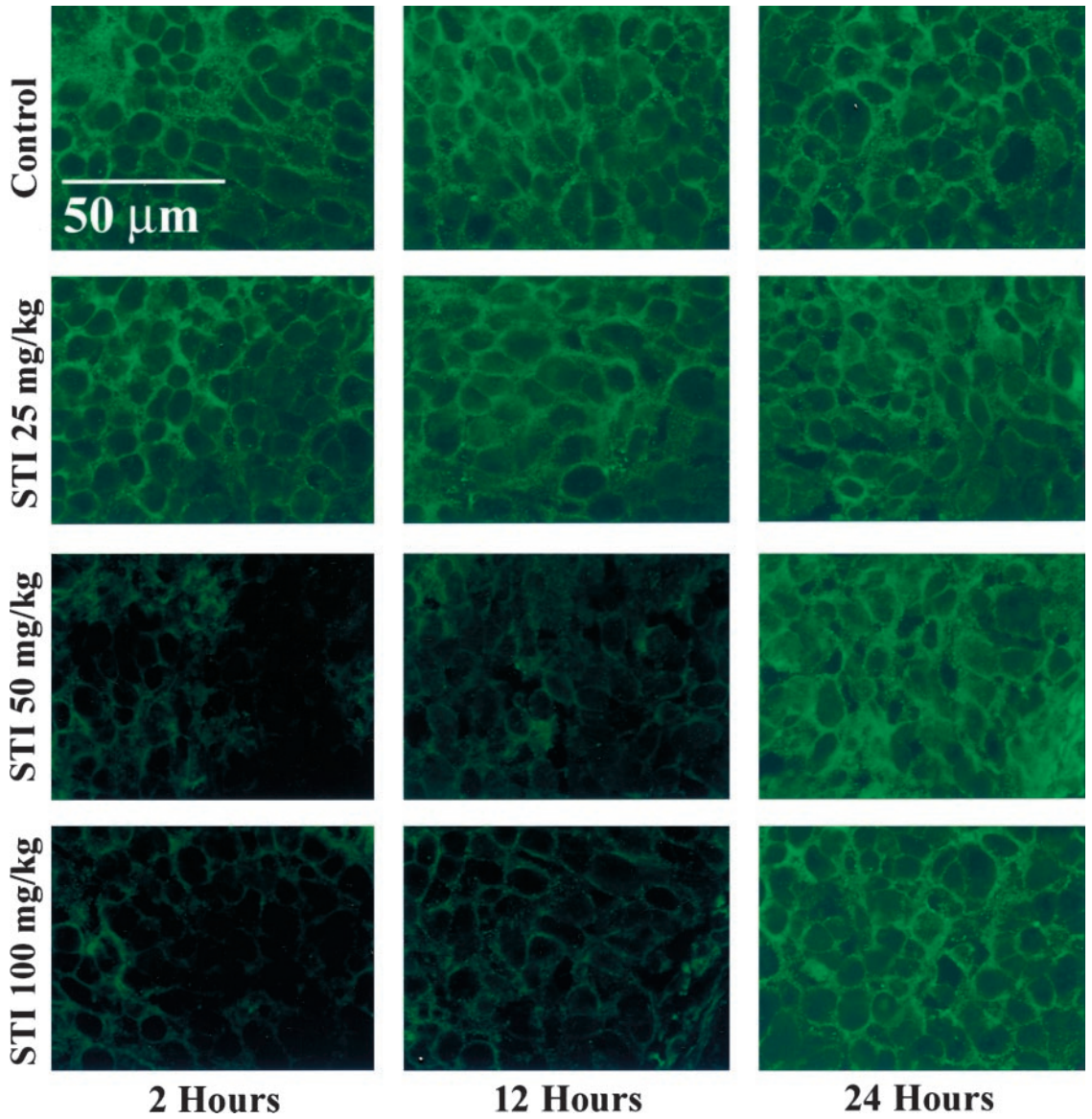

Fig. 1 Immunohistochemistry (IHC) analysis of SKOV3ip1 tumors growing in the peritoneal cavity of nude mice demonstrating the inhibition of phosphorylated platelet-derived growth factor receptor α expression (*green*) by STI571 *in vivo*. In separate experiments, the human ovarian carcinoma cell lines Hey A8 and SKOV3ip1 were implanted orthotopically in nude mice. Two weeks later, groups received STI571 at 0, 25, 50, and 100 mg/kg p.o. daily for 5 days. Tumors were harvested 2, 12, and 24 h after the day 5 dose.

other therapies, including paclitaxel alone ($P < 0.05$). The reduction in ascites found in both the paclitaxel-alone and STI571-paclitaxel combination groups was statistically significant compared with either control or STI571 treatments alone ($P < 0.01$). Body weight was maintained in mice that received either paclitaxel alone or the combination therapy, compared with control or STI571 alone ($P < 0.05$).

In the Hey A8 tumors (Table 2), STI571 had no therapeutic benefit over the saline control. However, the paclitaxel-STI571 combination therapy significantly reduced tumor incidence and tumor weight, compared with all other treatments ($P < 0.05$). For Hey A8 paclitaxel-resistant tumors (Table 3), STI571 alone was again ineffective. However, in contrast to findings from the previous two experiments, paclitaxel therapy alone was not effective in this highly paclitaxel-resistant cell line. The reduction in tumor weight among lesions treated with the combination of STI571 and paclitaxel was statistically significant compared with the other treatments ($P < 0.05$).

IHC Analysis. In the next set of experiments, we determined the mechanism(s) responsible for the therapeutic effects of STI571 plus paclitaxel. IHC analysis of SKOVip1, HEY A8, and HEY A8 paclitaxel-resistant tumors demonstrated that tumor-associated endothelial cells expressed PDGF-R and phosphorylated PDGF-R. The data shown in Fig. 2*A* are representative of HEY A8 tumors. The expression of PDGF-Rα was not reduced by any of the treatments. Fig. 2 also demonstrates that

Table 1 Therapy for SKOV3ip1 tumors implanted orthotopically in nude mice

Treatment group	Incidence[a]	Mean tumor weight ± SD (g)	Mean ascites (ml)	Mean body weight (g)
Control	10/10	1.0 ± 0.6	1.5	22.0
Paclitaxel	10/10	0.4[b] ± 0.2	0.0	25.4[b]
STI571	10/10	0.9 ± 0.5	1.4	22.1
Paclitaxel + STI571	7/10	0.1[c] ± 0.1	0.0[d]	24.7[d]

[a] Number of mice with tumor/number of mice injected.
[b] $P < 0.05$ compared with control and STI571 alone.
[c] $P < 0.05$ compared with all other groups, including paclitaxel alone.
[d] $P < 0.01$ compared with control and STI571 alone.

Table 2 Therapy for Hey A8 tumors implanted orthotopically into nude mice

Treatment group	Incidence[a]	Mean tumor weight ± SD (g)	Mean body weight ± SD (g)
Control	10/10	2.2 ± 0.9	24.4 ± 1.2
Paclitaxel	9/10	1.1[b] ± 0.7	23.8 ± 1.7
STI571	10/10	1.9 ± 0.8	24.1 ± 1.0
Paclitaxel + STI571	7/10	0.5[c] ± 0.4	24.5 ± 0.9

[a] Number of mice with tumor/number of mice injected.
[b] $P < 0.01$ compared with control and STI571 alone.
[c] $P < 0.05$ compared with all other groups, including paclitaxel alone.

endothelial cells in the tumors produced by Hey A8 cells expressed PDGF-Rα (yellow fluorescence). Fig. 2*B* demonstrates that tumor cells and endothelial cells expressed *p*-PDGF-R in mice treated with saline or paclitaxel alone. In mice treated with STI571 alone or with STI571 plus paclitaxel, the expression of *p*-PDGF-R by tumor cells and endothelial cells decreased. This figure also shows that tumor-associated endothelial cells expressed activated PDGF-R.

Next, we evaluated tumor cell and tumor-associated endothelial cell apoptosis using the TUNEL method. Using the double-labeled fluorescence technique, cells undergoing apoptosis, *i.e.*, TUNEL$^+$ cells, exhibit green fluorescence, and endothelial cells (CD31$^+$) stain red. Apoptotic endothelial cells have yellow nuclei. The data shown in Fig. 3*A* are from experiments using the paclitaxel-sensitive SKOV3ip1 and Hey A8 cell lines. Minimal tumor cell or endothelial cell apoptosis was apparent in either the control or single-agent STI571 treatment groups. The CD31/TUNEL column shows that for the paclitaxel-only group, tumor cells underwent apoptosis. In the combination therapy group, the CD31/TUNEL column shows yellow fluorescence, indicating that endothelial cells, in addition to tumor cells, underwent apoptosis. Data for the Hey A8 paclitaxel-resistant tumors are shown in Fig. 3*B*. Again, no apoptosis was evident in tumor cells from groups of mice treated with saline or single-agent STI571. Unlike the results for paclitaxel-sensitive cells in Fig. 3*A*, paclitaxel alone did not lead to apoptosis of tumor cells from this resistant line as expected. However, when the Hey A8 paclitaxel-resistant tumors were treated with the combination therapy, endothelial cells underwent apoptosis (yellow), as did some tumor cells (green). These data imply that the combination therapy can reduce tumor progression by an antivascular mechanism of action.

Additional support for this conclusion comes from the data shown in Tables 4 and 5. Data from experiments on both the SKOV3ip1 and Hey A8 paclitaxel-sensitive cells were pooled for reporting in Table 4. In the paclitaxel-sensitive experiments, the number of TUNEL$^+$ tumor cells and percentage of TUNEL$^+$ endothelial cells increased significantly from 10 ± 4 and 0% in the control group to 49 ± 17 ($P < 0.01$ *versus* control) and 10% ($P < 0.05$ *versus* all groups), respectively, in the combination therapy group. For the paclitaxel-resistant Hey A8 cells, the number of TUNEL$^+$ tumor cells and the percentage of TUNEL$^+$ endothelial cells increased significantly from 9 ± 4 and 0% in the control group to 37 ± 16 ($P < 0.05$ *versus* all groups) and 9% ($P < 0.05$ *versus* all groups), respectively, in the combination therapy group.

To further define the mechanism of action, we performed IHC for CD31 and PCNA. Representative data from the paclitaxel-sensitive (SKOV3ip1 and Hey A8) tumors are shown in Fig. 3*A*. Although MVD was reduced from the control level (46 ± 8) in tumors treated with only paclitaxel, the most significant reduction was in the combination therapy group, where MVD decreased to 15 ± 5 ($P < 0.05$ *versus* all groups). Similarly, PCNA was most significantly reduced from control (110 ± 12) in tumors from mice receiving both paclitaxel and STI571 ($P < 0.05$ *versus* all other groups). Fig. 3*B* shows similar IHC results but for tumors grown from the paclitaxel-resistant cells. Tumors from mice treated with only paclitaxel had no changes in MVD or PCNA compared with either the control or STI571-only groups. However, when paclitaxel was combined with STI571, we found significant reductions in both MVD and PCNA (to 21 ± 7 and 47 ± 11, respectively; $P < 0.05$ *versus* all groups for both CD31 and PCNA). The combination therapy also induced tumor necrosis.

Discussion

Blockade of the PDGF-R signaling pathway by p.o. STI571 combined with i.p. paclitaxel significantly inhibited tumorigenicity of human ovarian cancer cells implanted in the peritoneal cavity of nude mice and tumor progression. These effects were demonstrated in two paclitaxel-sensitive (SKOV3ip1 and Hey A8) cell lines and one paclitaxel-resistant (Hey A8 paclitaxel-resistant) cell line. STI571 alone did not reduce the growth of neoplasms. Paclitaxel reduced tumor weight by 50–60% in the paclitaxel-sensitive cell lines but not

Table 3 Therapy for Hey A8 paclitaxel-resistant tumors implanted orthotopically in nude mice

Treatment group	Incidence[a]	Mean tumor weight ± SD (g)	Mean body weight ± SD (g)
Control	10/10	2.0 ± 0.5	21.6 ± 0.8
Paclitaxel	10/10	1.6 ± 0.4	21.9 ± 1.1
STI571	10/10	1.7 ± 0.4	22.2 ± 1.7
Paclitaxel + STI571	7/10	0.7[b] ± 0.6	21.9 ± 1.2

[a] Number of mice with tumor/number of mice injected.
[b] $P < 0.05$ compared with all other groups.

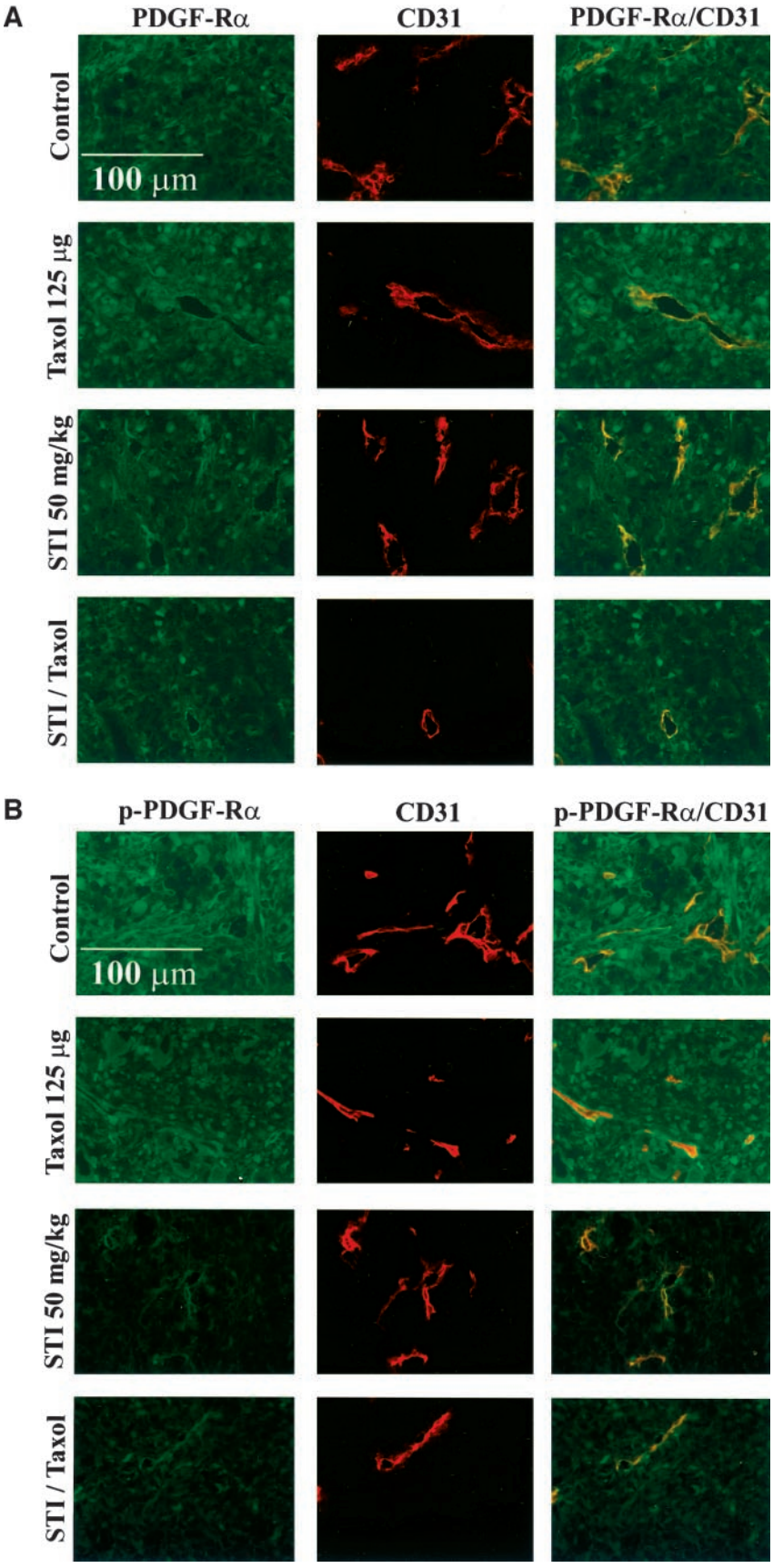

Fig. 2 Immunofluorescence double-labeling of HEY A8 ovarian carcinoma cells growing in the peritoneal cavity of nude mice. Groups of mice were treated with saline, paclitaxel (Taxol), STI571, or STI571 plus paclitaxel (Taxol). Tumors were harvested on day 45 and processed for immunohistochemistry. Representative images of fluorescence immunohistochemistry are shown for phosphorylated platelet-derived growth factor receptor α (PDGF-Rα), CD31, and the coexpression of CD31/PDGF-Rα (*A*); and phosphorylated (*p*)-PDGF-Rα, CD31, and the coexpression of CD31 and *p*-PDGF-Rα (*B*). Expression of PDGF-Rα and *p*-PDGF-Rα is shown in *green*; CD31 expression is in *red*. *Yellow* indicates coexpression of CD31 and the receptor. Note that expression PDGF-Rα and *p*-PDGF-Rα were expressed by tumor-associated endothelial cells and that of *p*-PDGF-Rα expression was downregulated in groups of mice that received STI571 alone or in combination with paclitaxel. PDGF-Rα expression was not affected by therapy.

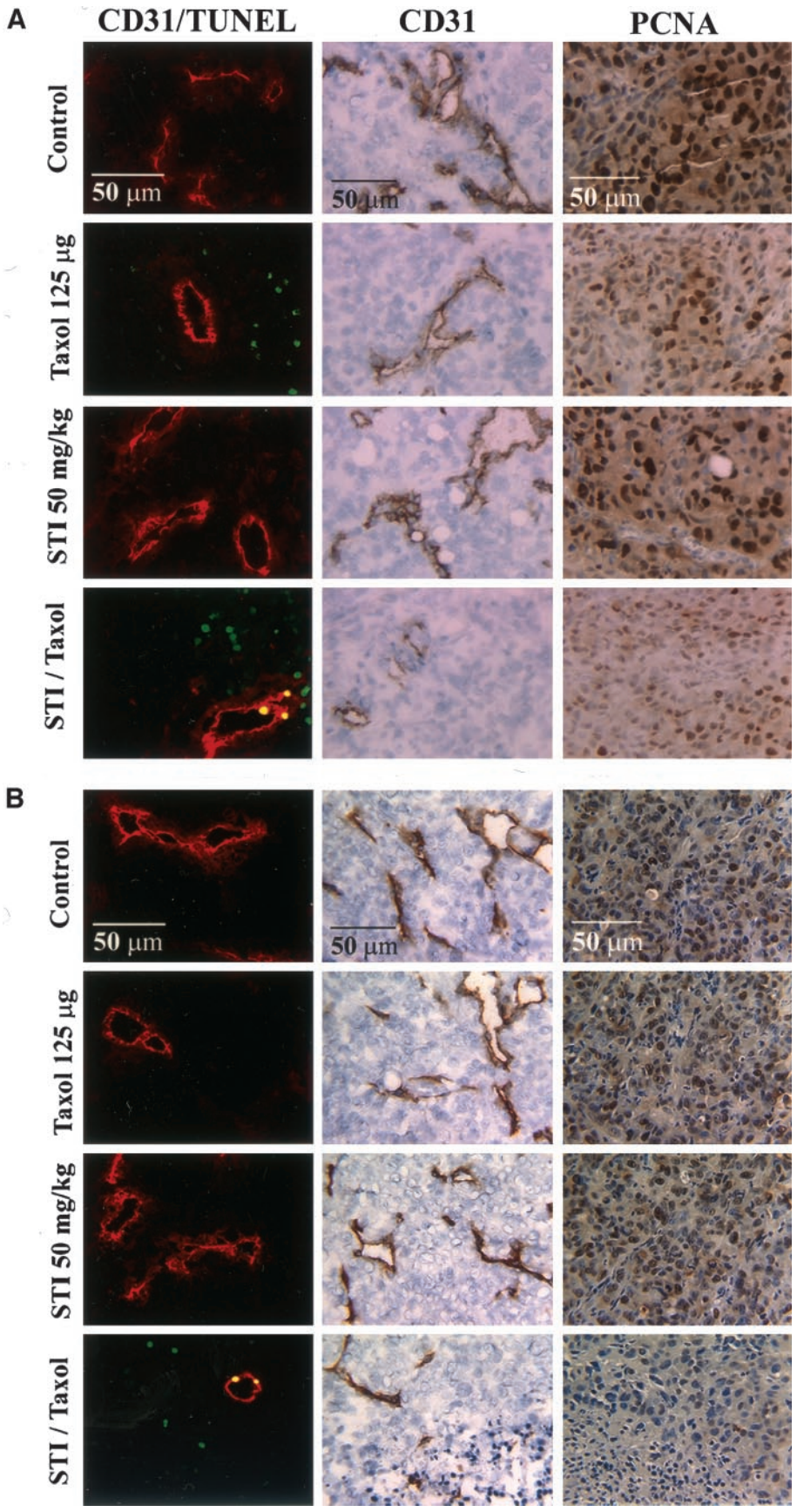

Fig. 3 Immunofluorescence and immunohistochemistry (IHC) of tumors derived from paclitaxel (Taxol)-sensitive cell lines SKOV3ip1 and Hey A8 (*A*), and Hey A8 paclitaxel (Taxol)-resistant human ovarian carcinoma cells growing in the peritoneal cavity of nude mice (*B*). Groups of mice were treated with saline, paclitaxel, STI571, or STI571 plus paclitaxel. Tumors were harvested on day 45 and processed for IHC. In the first column, representative images of fluorescence IHC show $CD31^+$ cells (*red*) and tumor cells undergoing apoptosis (*green*). *Yellow* indicates a $CD31^+$ cell that has undergone apoptosis. The second and third columns show representative results of colorimetric IHC analysis for CD31 and proliferating cell nuclear antigen (PCNA; shown in *brown*) for each treatment group in paclitaxel-sensitive (*A*) and resistant (*B*) tumors. Note the reduction in microvessel density and $PCNA^+$ cells as well as increased necrosis caused by the STI571-paclitaxel combination therapy.

Table 4 Immunohistochemical analysis of tumors from paclitaxel-sensitive human ovarian cancer cells SKOV3ip1 and Hey A8 growing in the peritoneal cavity of nude mice

Treatment group	CD31[a]	Proliferating cell nuclear antigen[a]	Tumor cells TUNEL^{+a}	Endothelial cells % TUNEL^{+b}
Control	46 ± 8	110 ± 12	10 ± 4	0
Paclitaxel	28 ± 7[c]	65 ± 16[c]	39 ± 15[c]	1
STI571	42 ± 6	106 ± 9	12 ± 7	0
Paclitaxel + STI571	15 ± 5[d]	35 ± 8[d]	49 ± 17[c]	10[d]

[a] Mean ± SD positive cells/field determined from quantitation in 10 random 0.159-mm^2 fields at ×100 magnification.
[b] Percentage of CD31$^+$ terminal deoxynucleotidyl transferase-mediated nick end labeling (TUNEL)$^+$ cells in 10 random 0.011-mm^2 fields at ×400 magnification.
[c] $P < 0.01$ compared with control and STI571 alone.
[d] $P < 0.05$ compared with all other groups, including paclitaxel alone.

in the paclitaxel-resistant cell line. In tumors from all three types, the combination of STI571 and paclitaxel significantly decreased tumor incidence and tumor weight. Prior studies from our laboratory determined that at the dose of 100 mg/kg, repeated daily administration of STI571 produced diarrhea and weight loss in nude mice (11). In our current study, the daily oral dose of STI571 (50 mg/kg) did not.

IHC analyses of tumors from all three of the cell lines showed that PDGF-R and *p*-PDGF-R were expressed by tumor-associated endothelial cells as well as tumor cells. PDGF-R and *p*-PDGF-R expression by tumor-associated endothelial cells suggests that blockade of receptor activation could affect endothelial cells as well as tumor cells. Investigations of apoptosis confirmed this. Tumors from paclitaxel-sensitive cell lines showed apoptosis of tumor cells with paclitaxel therapy and apoptosis of both tumor cells and endothelial cells with combination therapy. For tumors from the paclitaxel-resistant cells, tumor cell apoptosis was absent from the paclitaxel-only treatment group; however, endothelial cell apoptosis was observed when paclitaxel was combined with STI571. These data suggest that STI571-paclitaxel combination therapy reduced tumor weight by an antivascular mechanism of action.

The combination therapy-induced reduction in MVD and PCNA and the presence of necrosis provide additional evidence for an antivascular mechanism of action. Endothelial cell death would result in a disruption of existing tumor-associated vasculature and would inhibit new vessel formation, leading to hypoxia, decreased cell proliferation, and eventually necrosis; that is, endothelial cell death leads to tumor cell apoptosis. Neovascularization is a critical step in the metastatic cascade (39, 40), occurring both during the formation of the primary tumor mass and during the growth of metastases (11). The destruction of tumor-associated endothelial cells with combination paclitaxel-STI571 therapy could therefore reduce tumor burden and possibly prevent the outgrowth of metastases.

The reduction in tumor weight and induction of apoptosis in endothelial cells resulted from the addition of an agent that blocks the phosphorylation of PDGF-R. In effect, STI571 inhibited any autocrine or paracrine PDGF stimulation that the endothelial cells might have received. Yet, STI571 alone was not effective in reducing tumor weight, whereas the combination of STI571 and paclitaxel was superior to paclitaxel alone. Hence, the mere inhibition of PDGF-R activation was not sufficient to induce the death of endothelial cells. The blockade of PDGF-R activation increased the sensitivity of dividing tumor-associated endothelial cells to the effect of paclitaxel. That is, these data indicate that when the effects of PDGF are mitigated, the susceptibility of endothelial cells to paclitaxel-induced apoptosis is increased. Therefore, in this orthotopic model, PDGF functions as an antiapoptotic factor. These data are corroborated by other results characterizing PDGF as a survival or antiapoptotic factor (41–44). The death of tumor-associated endothelial cells leads to secondary tumor cell death and eventually tumor necrosis.

For the paclitaxel-resistant Hey A8 tumors, treatment with STI571 or paclitaxel alone failed to reduce tumor incidence or weight relative to control. In contrast, treatment using the combination of STI571 with paclitaxel was effective. This was

Table 5 Immunohistochemical analysis of tumors from paclitaxel-resistant Hey A8 human ovarian cancer cells growing in the peritoneal cavity of nude mice

Treatment group	CD31[a]	Proliferating cell nuclear antigen[a]	Tumor cells TUNEL^{+a}	Endothelial cells % TUNEL^{+b}
Control	48 ± 7	106 ± 8	9 ± 4	0
Paclitaxel	44 ± 6	99 ± 10	11 ± 6	1
STI571	46 ± 5	104 ± 9	10 ± 5	1
Paclitaxel + STI571	21 ± 7[c]	47 ± 11[c]	37 ± 16[d]	9[c]

[a] Mean ± SD positive cells/field determined from quantitation in 10 random 0.159-mm^2 fields at ×100 magnification.
[b] Percentage of CD31$^+$ terminal deoxynucleotidyl transferase-mediated nick end labeling (TUNEL)$^+$ cells in 10 random 0.011-mm^2 fields at ×400 magnification.
[c] $P < 0.05$ compared with all other groups.

probably due to the combination therapy's effect against the tumor-associated endothelial cells that were not resistant to paclitaxel. Unlike ovarian cancer cells, tumor-associated endothelial cells are genetically stable (45), and they are less likely than cancer cells to develop drug resistance. Moreover, compared with normal endothelial cells, tumor-associated endothelial cells undergo frequent cell division and should therefore be sensitive to chemotherapy. Compared with tumors, the turnover time of the normal-tissue endothelium is estimated to be 20–2000 times longer (46). A recent study suggested that continuous low-dose taxane-based therapy may be highly selective against cycling tumor-associated endothelial cells and that frequent low-dose regimens could potentiate antiangiogenic therapy (47). The fact that only the combination therapy was effective against tumors produced by paclitaxel-resistant cells suggests that the endothelial cells in the tumors were targeted for apoptosis. The data therefore suggest that the combination of STI571 and paclitaxel reduces ovarian cancer growth by an antivascular mechanism.

PDGF and PDGF-R have been shown to have important roles in angiogenesis and inhibition of apoptosis. PDGF-Rs are present on endothelial cells from various origins *in vitro* (48–50) and *in vivo* (51, 52). Several studies have suggested that PDGF might affect endothelial cells directly. PDGF-BB induced an angiogenic response in an assay system using the chorioallantoic membrane of the chick embryo (53, 54) in cultured rings of rat aorta (55) and in wound repair (56). Using tube-forming bovine aortic endothelial cells, PDGF-BB directly induced endothelial cell proliferation via PDGF-Rβ expressed on developing endothelial cords. Of note, PDGF-Rβ was absent from nonangiogenic endothelial cells (57). In addition to proliferation, PDGF-elicited endothelial cell migration has been observed in porcine aortic endothelial cells (58). PDGF-induced cell migration has also been shown in rat brain endothelial cells (53), rabbit retinal endothelial cells (58), and rabbit corneal endothelial cells (59, 60).

An indirect mechanism of action for PDGF-mediated angiogenesis has been suggested in several other studies. Blockade of PDGF-Rβ signals induced glomerular endothelial cell apoptosis in newborn mice (61). The results suggest that PDGF-Rβ pathways are particularly important for glomerular vasculogenesis in which endothelial cells actively undergo angiogenesis. Additional evidence for an indirect mechanism of action for PDGF in angiogenesis is provided by an analysis of pericytes. PDGFβ-chain produced by capillaries can recruit pericytes that are likely to be required to promote the structural integrity of the vessels (61–64). Taken together, these data demonstrate that PDGF can contribute to endothelial cell proliferation, migration, and remodeling.

Published studies show that PDGF potentially has an antiapoptotic function. PDGF is a principal survival factor that inhibits apoptosis and promotes proliferation (42), the mechanism of which involves activation of the Ras/PI3-K/Akt pathway (43, 44, 65). Nuclear factor-κB appears to be a target of the antiapoptotic Ras/PI3-K/Akt pathway (66). The antiapoptotic and proliferative effects of PDGF were shown in the *in vitro* MTT proliferation assay. Functional blockade of PDGF by STI571 resulted in a decrease of cellular proliferation. These data suggest a potential role for PDGF as a survival factor.

In addition to their effects on PDGF and PDGF-R on endothelial cells, several other mechanisms might explain the additive effects of STI571 and paclitaxel. Inhibition of PDGF-R signaling in tumor stroma has been shown to enhance the therapeutic effects of chemotherapy (67). That study suggested that the beneficial effect of cotreatment involves increased tumor uptake of chemotherapeutic agents, occurring most likely as a consequence of a reduction in the tumor interstitial fluid pressure. Moreover, STI571 and paclitaxel might have additive effects on microtubules. PDGF directly depolymerizes microtubules during the initiation of DNA synthesis and cell division (68, 69). STI571 inhibits PDGF-mediated PDGF-R activation and, hence, stabilizes microtubules in the target cells, a process similar to paclitaxel's mechanism of action; that is, paclitaxel promotes microtubule assembly (70). Thus, STI571 and paclitaxel might have additive effects on microtubule physiology.

Heterogeneous diseases such as cancer require multimodality therapies that target multiple biological mechanisms (45, 71). Paclitaxel is an effective, well-tolerated first-line agent in the chemotherapy armamentarium for ovarian cancer. Despite their tumors' high rate of initial response to paclitaxel therapy, many patients eventually develop paclitaxel-resistant tumors during the course of their disease. For this reason, a Hey A8 paclitaxel-resistant cell line was also developed and evaluated in this study. Therefore, an important aspect of this investigation was to determine any additive effects of STI571 in paclitaxel therapy. As expected, paclitaxel alone was not effective in the Hey A8 paclitaxel-resistant tumors; however, with the addition of STI571, the tumor-associated endothelial cells demonstrated apoptosis. Combination therapy worked by an antivascular mechanism; that is, blockade of PDGF-R activation sensitized the rapidly dividing, genetically stable, tumor-associated endothelial cells to paclitaxel-induced apoptosis. In effect, PDGF functioned as a survival factor. Tumor cell apoptosis was absent from the paclitaxel-only group, yet it was present in the combination therapy group; therefore, tumor-associated endothelial cell apoptosis may have contributed to secondary tumor cell death and, hence, effective therapy.

In summary, activation of the PDGF-R is important in the progression of ovarian cancer. Blockade of PDGF-R phosphorylation, in combination with paclitaxel-induced apoptosis, reduced tumor growth in an orthotopic nude mouse model by an antivascular mechanism of action. Inhibition of PDGF-R activation on endothelial cells renders these vital tumor components susceptible to paclitaxel-induced apoptosis. The data reported here thus are potentially significant for the design of a novel therapeutic approach for advanced or recurrent ovarian cancer.

Acknowledgments

We thank Kathryn Carnes for critical editorial comments and Lola López for expert assistance in the preparation of this manuscript.

References

1. Jemal, A., Murray, T., Samuels, A., Ghafoor, A., Ward, E., and Thun, M. J. Cancer statistics, 2003. CA - Cancer J. Clin., *53:* 5–26, 2003.

2. Oriel, K. A., Hartenbach, E. M., and Remington, P. L. Trends in United States ovarian cancer mortality, 1979–1995. Obstet. Gynecol., *93:* 30–33, 1999.

3. Cannistra, S. A. Cancer of the ovary. N. Engl. J. Med., *329:* 1550–1559, 1993.

4. McGuire, W. P., Hoskins, W. J., Brady, M. F., Kucera, P. R., Partridge, E. E., Look, K. Y., Clarke-Pearson, D. L., and Davidson, M. Cyclophosphamide and cisplatin compared with paclitaxel and cisplatin in patients with stage III and stage IV ovarian cancer. N. Engl. J. Med., *334:* 1–6, 1996.

5. Bookman, M. A., McGuire, W. P., III, Kilpatrick, D., Keenan, E., Hogan, W. M., Johnson, S. W., O'Dwyer, P., Rowinsky, E., Gallion, H. H., and Ozols, R. F. Carboplatin and paclitaxel in ovarian carcinoma: a Phase I study of the Gynecol. Oncol. Group. J. Clin. Oncol., *14:* 1895–1902, 1996.

6. Gore, M. E. Treatment of relapsed epithelial ovarian cancer. *In:* American Society of Clinical Oncology 2001 Education Book, pp. 468–476. Alexandria, VA: ASCO, 2001.

7. Fudge, K., Bostwick, D. G., and Stearns, M. E. Platelet-derived growth factor A and B chains and the α and β receptors in prostatic intraepithelial neoplasia. Prostate, *29:* 282–286, 1996.

8. Pirtskhalaishvili, G., and Nelson, J. B. Endothelium-derived factors as paracrine mediators of prostate cancer progression. Prostate, *44:* 77–87, 2000.

9. Sitaras, N. M., Sariban, E., Bravo, M., Pantazis, P., and Antoniades, H. N. Constitutive production of platelet-derived growth factor-like proteins by human prostate carcinoma cell lines. Cancer Res., *48:* 1930–1935, 1988.

10. Shawver, L. K., Schwartz, D. P., Mann, E., Chen, H., Tsai, J., Chu, L., Taylorson, L., Longhi, M., Meredith, S., Germain, L., Jacobs, J. S., Tang, C., Ullrich, A., Berens, M. E., Hersh, E., McMahon, G., Hirth, K. P., and Powell, T. J. Inhibition of platelet-derived growth factor-mediated signal transduction and tumor growth by *N*-[4-(trifluoromethyl)-phenyl]5-methylisoxazole-4-carboxamide. Clin. Cancer Res., *3:* 1167–1177, 1997.

11. Uehara, H., Kim, S., Karashima, T., Shepherd, D. L., Fan, D., Tsan, R., Killion, J. J., Logothetis, C., Mathew, P., and Fidler, I. J. Effects of blocking platelet-derived growth factor-receptor signaling in a mouse model of prostate cancer bone metastasis. J. Natl. Cancer Inst. (Bethesda), *95:* 558–570, 2003.

12. Antoniades, H. N., Galanopoulos, T., Neville-Golden, J., and O'Hara, C. J. Malignant epithelial cells in primary human lung carcinomas coexpress *in vivo* PDGF and PDGF-receptor mRNAs and their protein products. Proc. Natl. Acad. Sci. USA, *89:* 3942–3946, 1992.

13. Lindmark, G., Sundberg, C., Glimelius, B., Pahlman, L., Rubin, K., and Gerdin, B. Stromal expression of platelet-derived growth factor β-receptor and platelet-derived growth factor B-chain in colorectal cancer. Lab. Investig., *69:* 682–689, 1993.

14. Seymour, L., Dajee, D., and Bezwoda, W. R. Tissue platelet derived-growth factor (PDGF) predicts for shortened survival and treatment failure in advanced breast cancer. Breast Cancer Res. Treat., *26:* 247–252, 1993.

15. Yi, B., Williams, P. J., Niewolna, M., Wang, Y., and Yoneda, T. Tumor-derived platelet-derived growth factor-BB plays a critical role in osteosclerotic bone metastasis in an animal model of human breast cancer. Cancer Res., *62:* 917–923, 2002.

16. George, D. Platelet-derived growth factor receptors: a therapeutic target in solid tumors. Semin. Oncol., *28:* 27–33, 2001.

17. Fleming, T. P., Saxena, A., Clark, W. C., Robertson, J. T., Oldfield, E. H., Aaronson, S. A., and Ali, I. U. Amplification and/or overexpression of platelet-derived growth factor receptors and epidermal growth factor receptor in human glial tumors. Cancer Res., *52:* 4550–4553, 1992.

18. Guha, A., Dashner, K., Black, P. M., Wagner, J. A., and Stiles, C. D. Expression of PDGF and PDGF receptors in human astrocytoma operation specimens supports the existence of an autocrine loop. Int. J. Cancer, *60:* 168–173, 1995.

19. Ostman, A., and Heldin, C. H. Involvement of platelet-derived growth factor in disease: development of specific antagonists. Adv. Cancer Res., *80:* 1–38, 2001.

20. Dabrow, M. B., Francesco, M. R., McBrearty, F. X., and Caradonna, S. The effects of platelet-derived growth factor and receptor on normal and neoplastic human ovarian surface epithelium. Gynecol. Oncol., *71:* 29–37, 1998.

21. Henriksen, R., Funa, K., Wilander, E., Backstrom, T., Ridderheim, M., and Oberg, K. Expression and prognostic significance of platelet-derived growth factor and its receptors in epithelial ovarian neoplasms. Cancer Res., *53:* 4550–4554, 1993.

22. Versnel, M. A., Haarbrink, M., Langerak, A. W., de Laat, P. A., Hagemeijer, A., van der Kwast, T. H., van den Berg-Bakker, L. A., and Schrier, P. I. Human ovarian tumors of epithelial origin express PDGF *in vitro* and *in vivo.* Cancer Genet. Cytogenet., *73:* 60–64, 1994.

23. Druker, B. J., Tamura, S., Buchdunger, E., Ohno, S., Segal, G. M., Fanning, S., Zimmermann, J., and Lydon, N. B. Effects of a selective inhibitor of the Abl tyrosine kinase on the growth of Bcr-Abl positive cells. Nat. Med., *2:* 561–566, 1996.

24. Buchdunger, E., Cioffi, C. L., Law, N., Stover, D., Ohno-Jones, S., Druker, B. J., and Lydon, N. B. Abl protein-tyrosine kinase inhibitor STI571 inhibits *in vitro* signal transduction mediated by c-kit and platelet-derived growth factor receptors. J. Pharmacol. Exp. Ther., *295:* 139–145, 2000.

25. Ebert, M., Yokoyama, M., Friess, H., Kobrin, M. S., Buchler, M. W., and Korc, M. Induction of platelet-derived growth factor A and B chains and over-expression of their receptors in human pancreatic cancer. Int. J. Cancer, *62:* 529–535, 1995.

26. Druker, B. J., and Lydon, N. B. Lessons learned from the development of an Abl tyrosine kinase inhibitor for chronic myelogenous leukemia (Perspective). J. Clin. Investig., *105:* 3–7, 2000.

27. Druker, B. J., Talpaz, M., Resta, D., Peng, B., Buchdunger, E., Ford, J. M., Lydon, N. B., Kantarjian, H., Capdeville, R., Ohno-Jones, S., and Sawyers, C. L. Efficacy and safety of a specific inhibitor of the BCR-ABL tyrosine kinase in chronic myeloid leukemia. N. Engl. J. Med., *344:* 1031–1037, 2001.

28. Joensuu, H., Roberts, P. J., Sarlomo-Rikala, M., Andersson, L. C., Tervahartiala, P., Tuveson, D., Silberman, S. L., Capdeville, R., Dimitrijevic, S., Druker, B. J., and Demetri, G. D. Effect of the tyrosine kinase inhibitor STI571 in a patient with a metastatic gastrointestinal stromal tumor. N. Engl. J. Med., *344:* 1052–1056, 2001.

29. Sjoblom, T., Shimizu, A., O'Brien, K. P., Pietras, K., Dal Cin, P., Buchdunger, E., Dumanski, J. P., Ostman, A., and Heldin, C-H. Growth inhibition of dermatofibrosarcoma protuberans tumors by the platelet-derived growth factor receptor antagonist STI571 through induction of apoptosis. Cancer Res., *61:* 5778–5783, 2001.

30. Ahluwalia, A., Hurteau, J. A., Bigsby, R. M., and Nephew, K. P. DNA methylation in ovarian cancer. II. Expression of DNA methyltransferases in ovarian cancer cell lines and normal ovarian epithelial cells. Gynecol. Oncol., *82:* 299–304, 2001.

31. Buick, R. N., Pullano, R., and Trent, J. M. Comparative properties of five human ovarian adenocarcinoma cell lines. Cancer Res., *45:* 3668–3676, 1985.

32. Xu, L., and Fidler, I. J. Acidic pH-induced elevation in interleukin-8 expression by human ovarian carcinoma cells. Cancer Res., *60:* 4610–4616, 2000.

33. Yu, D., Wolf, J. K., Scanlon, M., Price, J. E., and Hung, M. C. Enhanced c-erbB-2/neu expression in human ovarian cancer cells correlates with more severe malignancy that can be suppressed by E1A. Cancer Res., *53:* 891–898, 1993.

34. Fogh, J., and Trempe, G. (eds.). Human Tumor Cells in Vitro. New York: Plenum Press, 1975.

35. Yoneda, J., Kuniyasu, H., Crispens, M. A., Price, J. E., Bucana, C. D., and Fidler, I. J. Expression of angiogenesis-related genes and progression of human ovarian carcinomas in nude mice. J. Natl. Cancer Inst. (Bethesda), *90:* 447–454, 1998.

36. Fan, D., Poste, G., Seid, C., Earnest, L. E., Bull, T., Clyne, R. K., and Fidler, I. J. Reversal of multidrug resistance in murine fibrosarcoma cells by thioxanthene flupentixol. Investig. New Drugs, *12:* 185–195, 1994.

37. Baker, C. H., Kedar, D., McCarty, M. F., Tsan, R., Weber, K. L., Bucana, C. D., and Fidler, I. J. Blockade of epidermal growth factor receptor signaling on tumor cells and tumor-associated endothelial cells for therapy of human carcinomas. Am. J. Pathol., *161:* 929–938, 2002.

38. Kim, S. J., Uehara, H., Karashima, T., Shepherd, D. L., Killion, J. J., and Fidler, I. J. Blockade of epidermal growth factor-receptor signaling in tumor cells and tumor-associated endothelial cells for therapy of androgen-independent human prostate cancer growing in the bone of nude mice. Clin. Cancer Res., *9:* 1200–1210, 2003.

39. Folkman, J. Angiogenesis in cancer, vascular, rheumatoid and other diseases. Nat. Med., *1:* 27–31, 1995.

40. Ellis, L. M., and Fidler, I. J. Tumor angiogenesis. *In:* J. Mendelsohn, P. M. Howley, M. A. Israel, and L. A. Liotta, (eds.), The Molecular Basis of Cancer, Ed. 2, pp. 173–185. Philadelphia: W. B. Saunders, 2001.

41. Harrington, E. A., Bennett, M. R., Fanidi, A., and Evan, G. I. c-Myc-induced apoptosis in fibroblasts is inhibited by specific cytokines. EMBO J., *13:* 3286–3295, 1994.

42. Kauffmann-Zeh, A., Rodriguez-Viciana, P., Ulrich, E., Gilbert, C., Coffer, P., Downward, J., and Evan, G. Suppression of c-Myc-induced apoptosis by Ras signaling through PI(3)K and PKB. Nature (Lond.), *385:* 544–548, 1997.

43. Kennedy, S. G., Wagner, A. J., Conzen, S. D., Jordan, J., Bellacosa, A., Tsichlis, P. N., and Hay, N. The PI 3-kinase/Akt signaling pathway delivers an anti-apoptotic signal. Genes Dev., *11:* 701–713, 1997.

44. Pietras, K., Sjöblom, T., Rubin, K., Heldin, C-H., and Östman, A. PDGF receptors as cancer drug targets. Cancer Cell, *3:* 439–443, 2003.

45. Fidler, I. J. The organ microenvironment and cancer metastasis (Review). Differentiation, *70:* 498–505, 2002.

46. Hobson, B., and Denekamp, J. Endothelial proliferation in tumours and normal tissues: continuous labeling studies. Br. J. Cancer, *49:* 405–413, 1984.

47. Bocci, G., Nicolson, K. C., and Kerbel, R. S. Protracted low-dose effects on human endothelial cell proliferation and survival *in vitro* reveal a selective antiangiogenic window for various chemotherapeutic drugs. Cancer Res., *62:* 6938–6943, 2002.

48. Bar, R. S., Boes, M., Booth, B. A., Dake, B. L., Henley, S., and Hart, M. N. The effects of platelet-derived growth factor in cultured microvessel endothelial cells. Endocrinology, *124:* 1841–1848, 1989.

49. Beitz, J. G., Kim, I. S., Calabresi, P., and Frackelton, A. R., Jr. Human microvascular endothelial cells express receptors for platelet-derived growth factor. Proc. Natl. Acad. Sci. USA, *88:* 2021–2025, 1991.

50. Marx, M., Perlmutter, R. A., and Madri, J. A. Modulation of platelet-derived growth factor receptor expression in microvascular endothelial cells during *in vitro* angiogenesis. J. Clin. Investig., *93:* 131–139, 1994.

51. Holmgren, L., Glaser, A., Pfeifer-Ohlsson, S., and Ohlsson, R. Angiogenesis during human extraembryonic development involves the spatiotemporal control of PDGF ligand and receptor gene expression. Development (Camb.), *113:* 749–754, 1991.

52. Plate, K. H., Breier, G., Farrell, C. L., and Risau, W. Platelet-derived growth factor receptor β is induced during tumor development and up-regulated during tumor progression in endothelial cells in human gliomas. Lab. Investig., *67:* 529–534, 1992.

53. Risau, W., Drexler, H., Mironov, V., Smits, A., Siegbahn, A., Funa, K., and Heldin, C. H. Platelet-derived growth factor is angiogenic *in vivo.* Growth Factors, *7:* 261–266, 1992.

54. Oikawa, T., Onozawa, C., Sakaguchi, M., Morita, I., and Murota, S. Three isoforms of platelet-derived growth factors all have the capability to induce angiogenesis *in vivo.* Biol. Pharm. Bull., *17:* 1686–1688, 1994.

55. Nicosia, R. F., Nicosia, S. V., and Smith, M. Vascular endothelial growth factor, platelet-derived growth factor, and insulin-like growth factor-1 promote rat aortic angiogenesis *in vitro.* Am. J. Pathol., *145:* 1023–1029, 1994.

56. Reuterdahl, C., Sundberg, C., Rubin, K., Funa, K., and Gerdin, B. Tissue localization of β receptors for platelet-derived growth factor and platelet-derived growth factor B chain during wound repair in humans. J. Clin. Investig., *91:* 2065–2075, 1993.

57. Battegay, E. J., Rupp, J., Iruela-Arispe, L., Sage, E. H., and Pech, M. PDGF-BB modulates endothelial proliferation and angiogenesis *in vitro* via PDGF β receptors. J. Cell Biol., *125:* 917–928, 1994.

58. Westermark, B., Siegbahn, A., Heldin, C. H., and Claesson-Welsh, L. B-Type receptor for platelet-derived growth factor mediates a chemotactic response by means of ligand-induced activation of the receptor protein-tyrosine kinase. Proc. Natl. Acad. Sci. USA, *87:* 128–132, 1990.

59. Koyama, N., Watanabe, S., Tezuka, M., Morisaki, N., Saito, Y., and Yoshida, S. Migratory and proliferative effect of platelet-derived growth factor in rabbit retinal endothelial cells: evidence of an autocrine pathway of platelet-derived growth factor. J. Cell. Physiol., *158:* 1–6, 1994.

60. Iguchi, I., Kamiyama, K., Wang, X., Kita, M., Imanishi, J., Yamaguchi, N., Sotozono, C., and Kinoshita, S. Enhancing effect of platelet-derived growth factors on migration of corneal endothelial cells. Cornea, *14:* 365–371, 1995.

61. Sano, H., Ueda, Y., Takakura, N., Takemura, G., Doi, T., Kataoka, H., Murayama, T., Xu, Y., Sudo, T., Nishikawa, S., Fujiwara, H., Kita, T., and Yokode, M. Blockade of platelet-derived growth factor receptor β pathway induces apoptosis of vascular endothelial cells and disrupts glomerular capillary formation in neonatal mice. Am. J. Pathol., *161:* 135–143, 2002.

62. Lindahl, P., Johansson, B. R., Leveen, P., and Betsholtz, C. Pericyte loss and microaneurysm formation in PDGF-B-deficient mice. Science (Wash. DC), *277:* 242–245, 1997.

63. Sundberg, C., Ljungstrom, M., Lindmark, G., Gerdin, B., and Rubin, K. Microvascular pericytes express platelet-derived growth factor-beta receptors in human healing wounds and colorectal adenocarcinoma. Am. J. Pathol., *143:* 1377–1388, 1993.

64. Crosby, J. R., Seifert, R. A., Soriano, P., and Bowen-Pope, D. F. Chimaeric analysis reveals role of PDGF receptors in all muscle lineages. Nat. Genet., *18:* 385–388, 1998.

65. Chaudhary, L. R., and Hruska, K. A. The cell survival signal Akt is differentially activated by PDGF-BB, EGF, and FGF-2 in osteoblastic cells. J. Cell. Biochem., *81:* 304–311, 2001.

66. Romashkova, J. A., and Makarov, S. S. NF-κB is a target of AKT in anti-apoptotic PDGF signaling. Nature (Lond.), *401:* 86–90, 1999.

67. Pietras, K., Rubin, K., Sjoblom, T., Buchdunger, E., Sjoquist, M., Heldin, C. H., and Ostman, A. Inhibition of PDGF receptor signaling in tumor stroma enhances antitumor effect of chemotherapy. Cancer Res., *62:* 5476–5484, 2002.

68. Yoon, S. Y., Tefferi, A., and Li, C. Y. Cellular distribution of platelet-derived growth factor, transforming growth factor β, basic fibroblast growth factor, and their receptors in normal bone marrow. Acta Haematol., *104:* 151–157, 2000.

69. Thyberg, J. The microtubular cytoskeleton and the initiation of DNA synthesis. Exp. Cell Res., *155:* 1–8, 1984.

70. Schiff, P. B., Fant, J., and Horwitz, S. B. Promotion of microtubule assembly *in vitro* by Taxol. Nature (Lond.), *277:* 665–667, 1979.

71. Fidler, I. J. The pathogenesis of cancer metastasis: the 'seed and soil' hypothesis revisited (Timeline). Nat. Rev. Cancer, *9:* 453–458, 2003.

Clinical Cancer Research

Targeting the Platelet-Derived Growth Factor Receptor in Antivascular Therapy for Human Ovarian Carcinoma

Sachin M. Apte, Dominic Fan, Jerald J. Killion, et al.

Clin Cancer Res 2004;10:897-908.